Genes & Genomics (2019) 41:1475–1492
https://doi.org/10.1007/s13258-019-00867-x

Online ISSN 2092-9293
Print ISSN 1976-9571

RESEARCH ARTICLE

Comparative transcript profiling and cytological observation of the newly bred recessive genic male sterility non-heading Chinese cabbage (*Brassica rapa* ssp. chinensis) line WS24-3A

Liping Song[1] · Xia Li[3] · Feng Zu[4] · Changbin Gao[1] · Bincai Wang[1] · Chufa Lin[1] · Jinxing Tu[2] · Aihua Wang[1] · Guolin Zhou[1]

Received: 16 May 2019 / Accepted: 30 August 2019 / Published online: 1 October 2019

Abstract

Background WS24-3A is a newly bred non-heading Chinese cabbage genic male-sterile line, in which sterility is controlled by a recessive gene, designated as *Bra2ms*. WS24-3A has been used for hybrid breeding.

Objective To reveal the underlying molecular mechanisms responsible for the sterility of WS24-3A.

Methods Cytological observation of the process of sterile/fertile anther development was performed to determine the tissue and stage in which sterility occurs. Phenotyping and transcriptomic analyses were performed to identify differentially expressed genes (DEGs) between sterile and fertile flower buds at different stages.

Results Cytological analysis revealed no tetrads at stage 7 or at later stages of anther development, and the degradation of callose was delayed. Abnormal meiocytes were surrounded by sustaining callose that degenerated gradually in WS24-3A. Comparative transcript profiling identified 3282 DEGs during three anther developmental stages, namely, pre-meiotic anther, meiotic anther, and anthers with single-celled pollen stage. The difference in DEG percentage between up-regulated and down-regulated at meiotic anther stage was obviously larger than at the other two stages; further, most DEGs are important for male meiosis, callose synthesis and dissolution, and tapetum development. Ten DEGs were found to be involved in anther and pollen development, which were analyzed by quantitative PCR.

Conclusion *Bra2ms* affected gene expression in meiocytes and associated with callose synthesis, degradation and tapetum development. Our results provide clues to elucidate the molecular mechanism of genic male sterility in non-heading Chinese cabbage.

Keywords Differentially expressed genes · Genic-male sterility · Non-heading Chinese cabbage

Introduction

In nature, male sterility is a common phenomenon in flowering plants and an effective strategy for the utilization of crop heterosis. In many crops, F_1 hybrids perform and yield better than their parents (Fu et al. 2014). For this purpose, genic male sterility (GMS) and cytoplasmic male sterility (CMS) have been applied for extensive production of hybrid seeds, as these traits produce seeds of high purity at low cost without intensive labor (Akter et al. 2016; Bohra et al. 2016). The whole process of anther development has been divided into 14 stages, including anther morphogenesis, microsporocyte division and differentiation, tetrad formation, callose and tapetum degradation, pollen grain development and maturation, anther dehiscence, and pollen grains release (Sanders et al. 1999). Anther development initiates with the

Liping Song and Xia Li have contributed equally to this work and share the first authorship.

Electronic supplementary material The online version of this article (https://doi.org/10.1007/s13258-019-00867-x) contains supplementary material, which is available to authorized users.

✉ Aihua Wang
wangaihualt@163.com

✉ Guolin Zhou
glzhou@126.com

Extended author information available on the last page of the article

differentiation of three cell layers, namely, L1, L2, and L3 at stage 1. The three cell layers gradually differentiate into four somatic cell layers, from the surface to the interior, namely epidermis, endothecium, middle layer, and tapetum. Reproductive cells and microspore mother cells develop between stages 2 and 5. Subsequently, microspore mother cells undergo meiosis during stage 6 and generate tetrads of haploid microspores at stage 7. Microspores are released from the tetrads at stage 8 and develop into mature pollen grains with three nucleus between stages 9 and 12 (Sanders et al. 1999). As the innermost somatic cell layer, tapetal cell differentiation and subsequent degradation coincide very well with the development of reproductive cells, and provide various nutrients for microspores, such as enzymes, lipids, and other molecules that are vital for normal microsporogenesis (Zhang and Yang 2014). Tapetal cells are formed at stage 5, they enter into the secretory phase at stage 6, function efficiently at stages 7–9, initiate degeneration via programmed cell death (PCD) at stage 10, and disappear after stage 11 (Sanders et al. 1999). Eventually, tapetal cell remnants are integrated into the pollen wall (Parish and Li 2010).

Anther development is controlled by a complex gene regulatory network that requires the coordinated activity of different tissues and cells derived from both sporophyte and gametophyte (Chang et al. 2011; Feng and Dickinson 2010; Hafidh et al. 2016; Ma 2006, 2013; Zhao 2009; Zhu et al. 2011). In *Arabidopsis thaliana*, there are approximately 3500 genes specifically expressed during anther development (Goldberg et al. 1993; Scott et al. 2004); additionally, several key genes controlling the differentiation and function of tapetal cells and meiosis of meiocytes have been cloned and elaborated (Cui et al. 2016; Glover et al. 1998; Hird et al. 1993; Ito et al. 2004; Lu et al. 2014; Schiefthaler et al. 1999; Yang et al. 2003b; Zhu et al. 2008, 2015). *SPOROCYTELESS/NOZZLE*(*SPL/NZZ*) encoding a putative transcription factor plays a central role in specification of both reproductive cells and somatic cells in early anther development (Schiefthaler et al. 1999). The endothecium, middle layer, tapetum, and meiocytes were absent in *spl/nzz* mutant anthers. *DYSFUNCTIONAL TAPETUM 1* (*DYT1*) encoding a putative bHLH transcription factor acts downstream of *SPL* and upstream of *Defective in Tapetal Development and Function 1* (*TDF1*), a transcription factor essential for tapetum development. *DYT1*, which preferentially expressed in tapetal cells and at a lower level in meiocytes, is a crucial component of a genetic network that regulates tapetum development. The *dyt1* mutant showed premature vacuolation of the tapetum and often failed to complete meiotic cytokinesis (Cui et al. 2016; Feng et al. 2012; Li et al. 2017; Zhang et al. 2006). *TDF1* encoding a putative R2R3 MYB transcription factor plays a vital role in tapetal cell differentiation and function, and preferentially expresses in both tapetal cells and meiocytes between stage 5 and stage 7. Tapetal cells were unable to change into the secretory tapetum and the tetrads failed to be released into the locule in *tdf1* mutant (Zhu et al. 2008). *DUET* (also known as *MALE MEIOCYTE DEATH 1*, *MMD1*) encoding a PHD-finger protein, is expressed preferentially in meiocytes at stage 6 and is required for meiotic chromosome organization and progression during meiosis of meiocytes. The *mmd1* mutation disrupted male meiosis and triggered cell death in male meiocytes at meiotic prophase I, finally no tetrads were produced in the *mmd1* mutant (Reddy et al. 2003; Wang et al. 2016b; Yang et al. 2003b). As a direct target of *DUET*, *TDM1* encodes a tetratricopeptide repeat protein required for determining the number of meiotic divisions. The *tdm1* mutant produced polyads or dyads of spores, depending on the mutation site (Andreuzza et al. 2015; Cifuentes et al. 2016; Glover et al. 1998).

In developing anthers of angiosperms, callose is a linear β-1, 3-glucan molecule. A specialized temporary cell wall consisting of callose was synthesized between the primary cell wall and the plasma membrane in microsporocytes. *CALS5* was the most important gene responsible for callose deposition surrounding meiocytes (Dong et al. 2005). *A6* is a significant component of the callose mixture secreted by the tapetum. *CDM1*, encoding a CCCH-type zinc finger protein, regulates callose metabolism in male meiocytes during micriosporogenesis and the *cdm1* mutation affects the expression of *CALS5* and *A6* (Lu et al. 2014). The C3Hs are a large family of zinc finger TFs that may function in RNA processing by binding RNA (Wang et al. 2008).

Non-heading Chinese cabbage (NHCC; *Brassica rapa* ssp. chinensis, 2n = 2x = 20) is one of the most economically important green leafy-vegetables worldwide, especially in China, with significant economic value. Non-heading Chinese cabbage is a typical cross-pollinated crop with obvious heterosis. In recent years, GMS has been used for breeding of non-heading Chinese cabbage. However, the underlying molecular mechanism for GMS in this species remains unclear. Recently, as the whole genome of *Brassica rapa* was sequenced and annotated (Wang et al. 2011), RNA-seq was successfully used to identify differentially expressed genes (DEGs) between fertile and sterile buds/anthers in *Brassica rapa*, which allowed us to gain an insight into the mechanism of sterility (Chang et al. 2016; Chen et al. 2018). In a previous study, we generated the genic male-sterility line WS24-3A of non-heading Chinese cabbage and its maintainer line, WS24-3B. Male sterility of WS24-3A was found to be controlled by one recessive gene locus designated as *Bra2ms* (Li et al. 2016). In this study, we performed comparative transcript profiling and microsection observation of fertile and sterile buds using the WS24-3A/B lines. The results of this work will contribute to our understanding of the mechanism underlying male sterility in this line and

provide helpful information for further gene cloning of *Bra2ms* in WS24-3A.

Materials and methods

Plant materials

WS24-3A is a newly reported genic male-sterile line, whose sterility is controlled by one recessive gene locus designated as *Bra2ms* (Li et al. 2016). For this study, we used the recessive genic male-sterile (RGMS) two-type line, WS24-3AB (*Bra2msBra2ms/Bra2MsBra2ms*), which was sib-mated for five generations. The line was sown and grown at Huazhong Agriculture University (Wuhan, Hubei Province, China). After flowering, male fertile plants, WS24-3B (*Bra2Ms-Bra2ms*), and male sterile plants, WS24-3A (*Bra2ms-Bra2ms*), were easily distinguished from one to another (Fig. S1) and flower buds were stripped from at least 10 different plants for transcriptomic analysis. Buds were separately divided into three pools for sterile and fertile plants according to developmental stage (Table 1), snap-frozen in liquid nitrogen, and kept at − 80 °C for total RNA extraction.

Semi-thin sections and light microscopy

Sterile and fertile flower buds were harvested and directly fixed in FAA (10 ml formalin, 3 ml acetic acid, and 87 ml of 50% ethanol) for 24 h at the initial stages of flower development. Then, samples were dehydrated through a series of graded ethanol solutions (50%, 70%, 90%, and 100%), and embedded in resin using a Technovit Embedding Kit (Germany). Semi-thin (2.0 µm) sections were obtained using an automatic microtome (Microm HM 360, Thermo Scientific). Selected sections were stained with 0.1% toluidine blue (Sigma-Aldrich) for 10 s at room temperature and observed with a Nikon Eclipse 80i microscope (Nikon, Japan). Images of the anthers at different developmental stages were captured with a Nikon DS-Ri1 camera (Nikon, Japan). For observation of fluorescence expression of callose, sections were stained with aniline blue and micrographs were taken using a fluorescence microscope (Nikon Eclipse 80i) with the appropriate filter under ultraviolet light.

RNA Isolation, cDNA library construction and illumina sequencing

Total RNA was extracted with the TRIzol kit (Invitrogen, USA) according to manufacturer instructions and purified using an mRNA purification kit (Promega, China) following the protocol suggested by the manufacturer. mRNA was reverse transcribed by Powderscript™ II (Takara, China). Double-stranded cDNA was amplified using a random hexamer, DNA polymerase I and RNase H, and purified using a DNA purification kit (QIAGEN, Germany). Finally, cDNA libraries were prepared from a 300–500 bp size-selected fraction following agarose gel separation and adapter ligation for final Illumina sequencing. The libraries were sequenced using a paired-end read protocol with 125 bp of data collected per run on the Illumina Hiseq 2000 platform.

Analysis of illumina sequencing results

Clean reads were obtained from raw data by filtering adaptor sequences and low-quality sequences as previously described (Wang et al. 2016a). Then, sequence reads were aligned to the reference genome (http://brassicadb.org/brad/) using Tophat (Trapnell et al. 2010). Following alignments, the number of reads mapped to each *Brassica rapa* gene model was derived and normalized by the FPKM (fragments per kilobase of exon per million fragments mapped) method using Cufflinks (Trapnell et al. 2012).

Identification of differentially expressed genes (DEGs)

Differentially expressed genes between male fertile and male sterile flower buds at different developmental stages were identified with the DESeq package (Wang et al. 2010). A combination of FDR (false discovery rate) value ≤ 0.01 and the absolute value of $\log_2$ (fold-change) ≥ 1 were used as threshold to estimate the significance of the difference in gene expression.

Table 1 Description of floral buds used in the transcriptome analysis performed

Bud samples	Bud size	Pollen developmental stage
Sterile buds		
S1	< 0.8 mm	PMA(Pre-meiotic anther, stage 1–5)
S2	0.8 ≤ buds < 1.5 mm	MAT(Meiotic and tetrad anther, stage 6–7)
S1	1.5 ≤ buds < 2.5 mm	SCP(Anther with single celled pollen, stage 8–9)
Fertile buds		
F1	<0.8 mm	PMA(Pre-meiotic anther, stage 1–5)
F2	0.8 ≤ buds < 1.5 mm	MAT(Meiotic and tetrad anther, stage 6–7)
F3	1.5 ≤ buds < 2.5 mm	SCP(Anther with single celled pollen, stage 8–9)

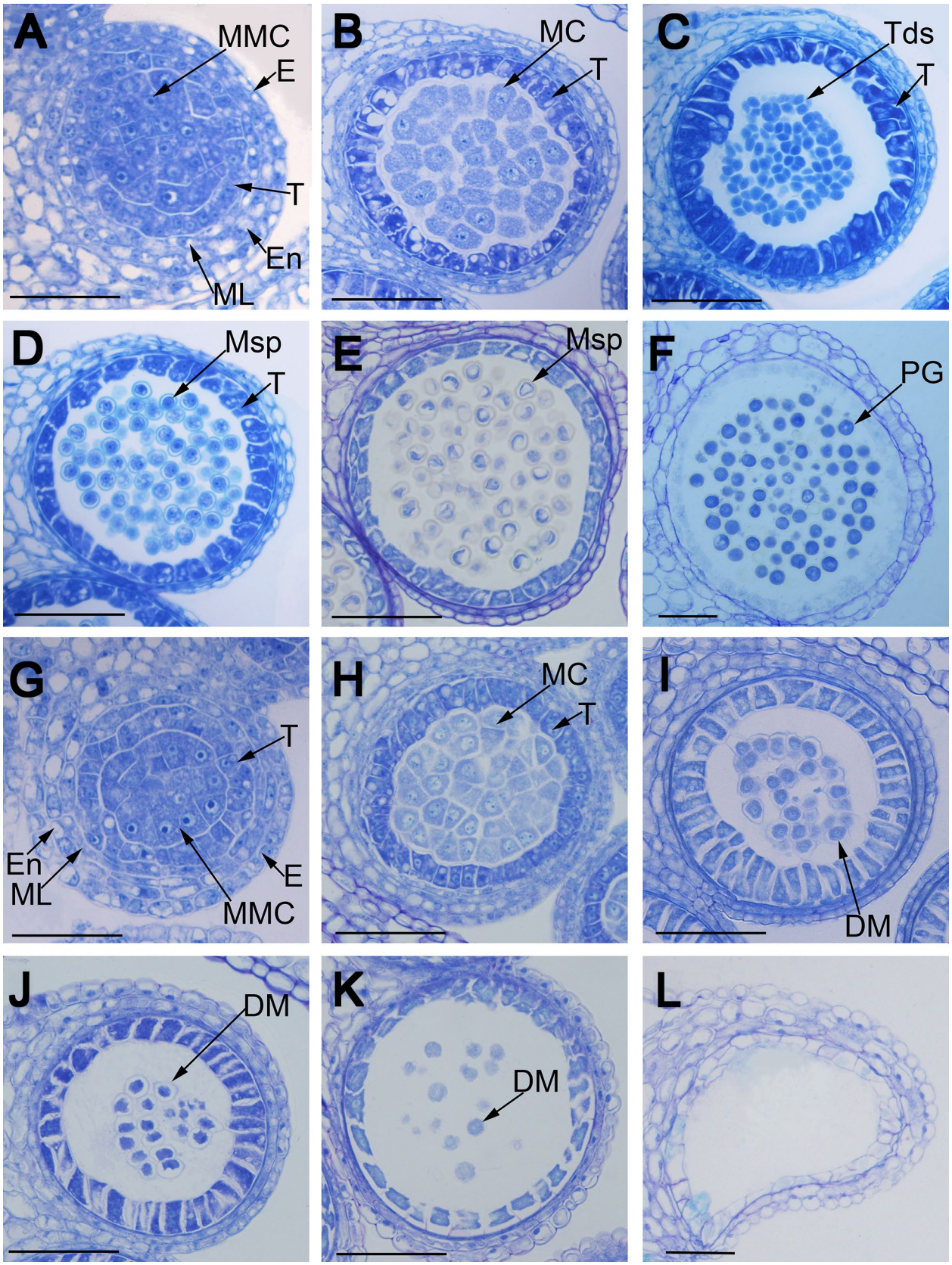
A
MMC
E
T
En
ML
B
MC
T
C
Tds
T
D
Msp
T
E
Msp
F
PG
G
T
En
ML
E
MMC
H
MC
T
I
DM
J
DM
K
DM
L

◂**Fig. 1** Pollen development in fertile (**a**–**f**) and sterile (**g**–**l**) Chinese cabbage anthers. Stage 5 (**a**, **g**), stage 6 (**b**, **h**), stage 7 (**c**, **i**), stage 8 (**d**, **j**), stage 9 (**e**, **k**) and stage 11 (**f**, **l**). *DM* degenerating meiocytes, *E* epidermis, *En* endothecium, *MC* meiotic cell, *ML* middle layer, *MMC* microspore mother cell, *Msp* microspore, *PG* pollen grain, *T* tapetum, *Tds* tetrads. Scale bar 50 μm

The orthologs of these DEGs in *Arabidopsis thaliana* were retrieved from BRAD (http://brassicadb.org/brad/). After data normalization, hierarchical clustering analysis of the expression patterns was performed by MeV software (http://www.tm4.org/mev.html).

GO and KEGG enrichment analysis

To identify putative biological functions and pathways of identified DEGs, Blast2Go (Gotz et al. 2008) and KOBAS (Xie et al. 2011) (http://kobas.cbi.pku.edu.cn/home.do) were used to perform GO and KEGG annotation and enrichment, respectively. WEGO (http://wego.genomics.org.cn/) was used to plot GO annotation (Ye et al. 2006). GO functional enrichment and KEGG pathway enrichment analysis were tested at a significance cutoff of 0.05 FDR.

Real-time PCR (qRT-PCR) validation

For real time quantitative RT-PCR, 1 μg total RNA was used to synthesize the first-strand cDNA using the RevertAid First Strand cDNA Synthesis Kit (Thermo Scientific). Gene-specific primers were designed based on the selected DEGs sequences. Reactions were performed with the SYBR Green Realtime PCR Master Mix (TOYOBO, Japan) in a Bio-Rad CFX96 instrument. The RT-PCRs were carried out with following protocol: 95 °C for 10 min, followed by 40 cycles of 95 °C for 15 s, and 60 °C for 60 s. Three biological replicates for each sample and three technical replicates for each biological replicate were analyzed. Significant differences of gene expression level between male fertile and sterile flower buds were evaluated using a Student's t-test. *BrActin7* (XM_009127097) was used as internal control to normalize gene expression.

Availability of supporting data

Supporting data sets are included in the Supplementary Online Materials. Sequencing raw data have been deposited in an SRA database at the NCBI under accession number SRP095649.

Results

Phenotypic characteristics of fertile and sterile flower buds

No significant differences were observed between fertile and sterile buds at the initial stage of flower bud development. Subsequently, anthers and filaments of sterile buds showed growth arrest. Finally, sterile anthers produced no mature pollen and the filaments were markedly shorter than those in fertile flowers, although the pistil of sterile flowers appeared normal (Fig. S1).

To accurately determine the tissue and stage in which sterility occurs, the process of sterile/fertile anther development was observed by cytological microscopic techniques. As shown in Fig. 1, there was no obvious difference between sterile and fertile anthers at stage 5 of development, at which, microspore mother cells (MMCs) developed normally in both fertile and sterile anthers, surrounded by the tapetum, middle layer, endothecium, and epidermis from the innermost to the outermost layer (Fig. 1a, g). However, entering the meiotic period (stage 6), MMCs in sterile anthers exhibited larger vacuoles and less concentrated nuclei, with less staining than those of fertile anthers (Fig. 1b, h). Tetrads formed in fertile anther at the end of meiosis (stage 7); tapetal cells walls degraded; tapetal cells shrank and were stained deeply (Fig. 1c). Then, with the gradual degradation of callose surrounding the tetrads, separated microspores were released into the locules and further developed into mature pollen grains at stage 11 in fertile anthers (Fig. 1d, e, f). In contrast, no tetrads were observed in sterile anther at that stage or later. This indicated that MMCs were unable to complete meiosis (Fig. 1i, j), with tapetal cell walls remaining intact and visible and tapetal cells containing more vacuoles with less staining at stage 7 (Fig. 1i), which means that tapetal cells failed to transform into secretory cells. Subsequently, these abnormal meiocytes surrounded by callose degenerated gradually, and finally no mature pollen was produced (Fig. 1j, k).

In order to further understand the abnormalities of callose dissolution in sterile anthers, fertile and sterile anther sections from different developmental stages were stained with aniline blue and observed under ultraviolet light. At meiosis (stage 6) callose fluorescence was observed in both locules of fertile and sterile anthers (Fig. 2a, e), and the fluorescence signal became clearest at the tetrad stage (Fig. 2b, f), after which, the signal remained to be observed in sterile anthers (Fig. 2g, h), but not in fertile anthers (Fig. 2c, d). These results indicated that degradation of callose was delayed in sterile anthers.

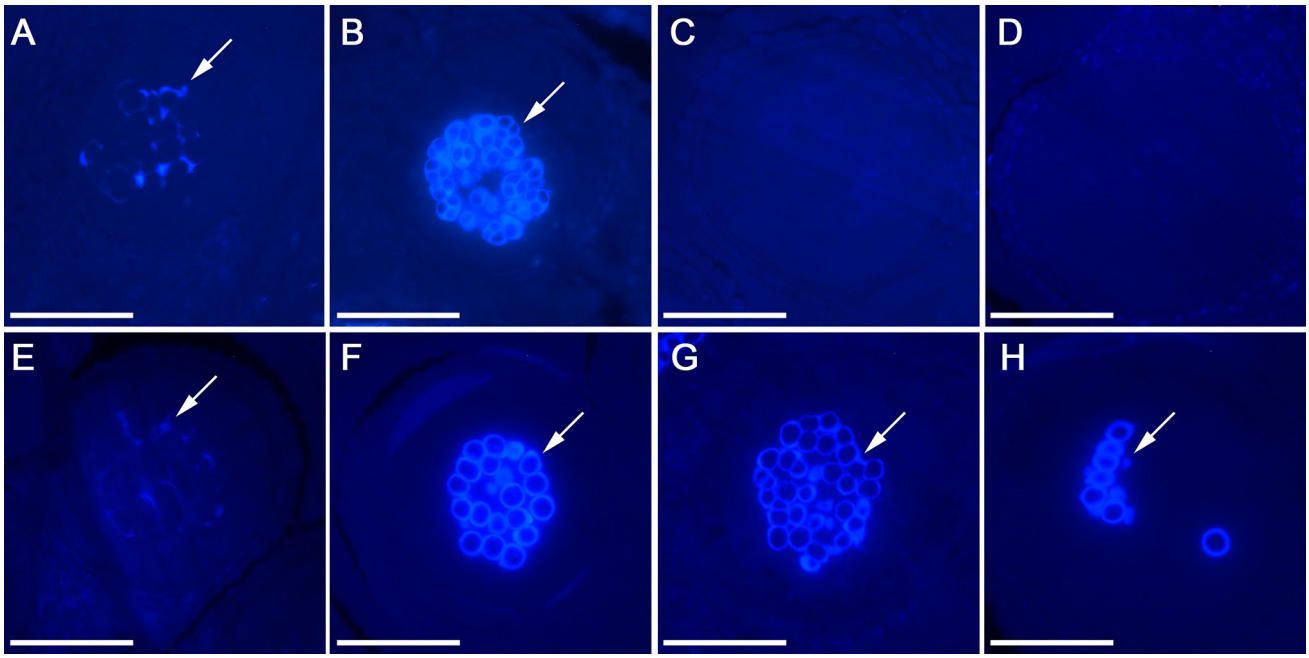

Fig. 2 Analysis of callose dissolution in fertile (**a**–**d**) and sterile (**e**–**h**) Chinese cabbage anthers. Stage 6 (**a**, **e**), stage 7 (**b**, **f**), stage 8 (**c**, **g**), and stage 9 (**d**, **h**)

cDNA library construction and overview of RNA sequencing

According to the morphological features of fertile anthers and the corresponding floral bud size, fertile and sterile buds were divided separately into three distinct stages, pre-meiotic anther (PMA), meiotic anther (MA) and anthers with single-celled pollen (SCP). S1, S2 and S3 are samples of stages PMA, MA and SCP for sterile buds, while F1, F2 and F3 are samples of the corresponding stage in fertile buds, respectively (Table 1).

At each stage, fertile and sterile buds were further divided separately into two pools as two biological repeats for constructing cDNA libraries. In all, 12 libraries of fertile and sterile buds were created for RNA-seq. After quality control, approximately 435 million paired-end reads were obtained (Table 2). Of the total clean reads, an average of 75.02% of these reads were mapped to the reference *B. rapa* genome by Tophat, and a total 41020 predicted genes were annotated.

Table 2 Summary of alignment statistics of RNA-Seq in 12 libraries mapped to *B. rapa* reference genome

	Total reads	Total mapped reads	Unique match	Multi-position match	Unmapped reads
S1_rep1	39,204,504	29,228,949 (74.56%)	27,851,909 (71.04%)	1,377,040 (3.51%)	9,975,555 (25.44%)
S1_rep2	37,577,024	27,997,692 (74.51%)	26,744,777 (71.17%)	1,252,915 (3.33%)	9,579,332 (25.49%)
S2_rep1	38,531,068	29,080,229 (75.47%)	27,755,276 (72.03%)	1,324,953 (3.44%)	9,450,839 (24.53%)
S2_rep2	35,201,232	26,531,594 (75.37%)	25,388,601 (72.12%)	1,142,993 (3.25%)	8,669,638 (24.63%)
S3_rep1	36,245,818	26,967,286 (74.40%)	25,871,917 (71.38%)	1,095,369 (3.02%)	9,278,532 (25.60%)
S3_rep2	35,781,458	26,856,585 (75.06%)	25,699,474 (71.82%)	1,157,111 (3.23%)	8,924,873 (24.94%)
F1_rep1	38,846,040	28,825,569 (74.20%)	27,403,609 (70.54%)	1,421,960 (3.66%)	10,020,471 (25.80%)
F1_rep2	32,945,598	24,415,191 (74.11%)	23,152,616 (70.28%)	1,262,575 (3.83%)	8,530,407 (25.89%)
F2_rep1	37,967,074	28,623,501 (75.39%)	27,416,782 (72.21%)	1,206,719 (3.18%)	9,343,573 (24.61%)
F2_rep2	32,773,484	24,768,371 (75.57%)	23,712,497 (72.35%)	1,055,874 (3.22%)	8,005,113 (24.43%)
F3_rep1	38,468,910	29,177,078 (75.85%)	28,007,509 (72.81%)	1,169,569 (3.04%)	9,291,832 (24.15%)
F3_rep2	31,633,624	23,963,736 (75.75%)	22,899,904 (72.39%)	1,063,832 (3.36%)	7,669,888 (24.25%)

S1-rep1 and S1_rep2 are two biological repeats of S1 sample, so do the others

Global analysis and functional classification of DEGs

One of the basic goals of transcriptome study was to perform a global comparative analysis to obtain DEGs between sterile and fertile flower buds at different stages. In this study, 3282 genes (|log2 (fold-change)| ≥ 1, FDR ≤ 0.001) exhibited expression changes during the three anther developmental stages, PMA, MA and SCP, in sterile compared with fertile buds (Table S1). Among these genes, 1625 were up-regulated and 2055 were down-regulated during the three developmental stages, including 199 genes that showed regulated fluctuations across different stages. There were 25 and 26 DEGs up- and down- regulated, respectively, in all three stages. Moreover, comparative analysis of the number of stage-specific genes, between up- and down- regulated genes clusters, showed that the number of MA-specific genes in the down-regulated gene cluster (463) was significantly larger than the number in up-regulated gene cluster (144). However, there were no such obvious difference observed at the other two stages (Fig. 3a). Statistics of DEGs at different stages revealed that the number of DEGs increased with the anther development. There were 227 DEGs (119 up-regulated and 98 down-regulated), 908 DEGs (282 up-regulated and 626 down-regulated) and 2555 DEGs (1224 up-regulated and 1331 down-regulated) at PMA, MA and SCP stages, respectively. The difference in DEG percentage between up-regulated (282, 31%) and down-regulated (626, 69%) at MA stage was obviously larger than those at the other two stages (Fig. 3b). The heat-map of hierarchical cluster of 3282 DEGs was shown in Fig. 4. The correlations of different samples showed that S1 and F1, S2 and S3 had a closer relationship and F3 was most distant from other samples (Fig. 4). Among these 3282 DEGs, 2522 had corresponding orthologous genes in *Arabidopsis thaliana* according to the retrieval from BRAD (http://brassicadb.org/brad/) (Table S1).

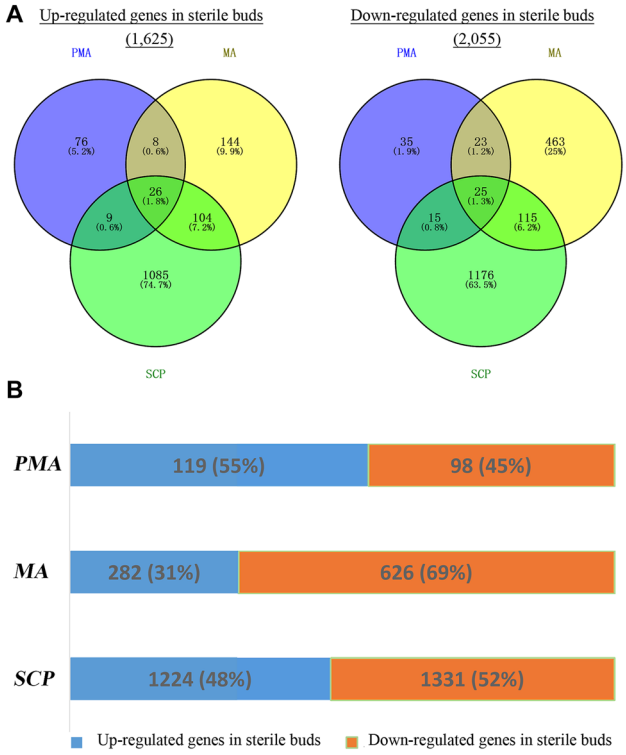

Fig. 3 Distribution of differentially expressed genes (DEGs) in three stages of anther development. **a** Venn diagram of distribution of DEGs at the three stages according to up- or down-regulated genes in sterile buds; **b** percentage packing column chart of DEGs for the three stages of anther development

To explore the information of functional annotation, all DEGs were aligned against the Gene Ontology (GO) (Ashburner et al. 2000) and the Kyoto Encyclopedia of Genes and Genomes (KEGG) (Kanehisa et al. 2008) database. For GO analysis, all DEGs were annotated into three major categories: Cell Component (CC), Molecular Function (MF) and Biological Process (BP), which were further classified into 45 GO subcategories (Fig. 5). The GO patterns of up- and down- regulated genes were very similar, except that the GO: 0015457 (auxiliary transport protein) only occurred in the up-regulated genes and the GO: 0001906 (cell killing) only occurred in the down-regulated genes. KEGG analysis showed that 95 and 117 categories were involved in up- and down- regulated genes, respectively, including metabolic pathways, biosynthesis of secondary metabolites, starch and sucrose metabolism and others. The top 10 KEGG pathway categories in either up- or down- regulated genes (Fig. 6).

Expression analysis of meiosis-related genes preferentially expressed in meiocytes

The observation of microsections showed that no tetrads were formed in sterile anthers at stage 7 (Fig. 1i). This suggested that sterility of WS24-3A might be linked with differential expression of meiosis-related genes, which are preferentially expressed in meiocytes. In *Arabidopsis*, 296 potential meiosis-related genes were identified by comparing meiocyte transcriptomes to those obtained from root tips and leaves, and further crossing with the set of down-regulated genes in *spl* mutant anthers (Libeau et al. 2011). Of these, 88 genes corresponding to 112 orthologous genes in *Brassica rapa* exhibited differential expression during the three anther developmental stages in sterile anther (Table S2). Among these genes, 20 and 2 were up-regulated and down-regulated at the PMA stage, respectively. In contrast, 43 genes were down-regulated, whereas only 1 gene was up-regulated at MA stage in sterile flower buds. At SCP stage, 13 and 48 genes were up-regulated and down-regulated in sterile flower buds, respectively. There was a marked enrichment of meiosis-related genes among down-regulated genes

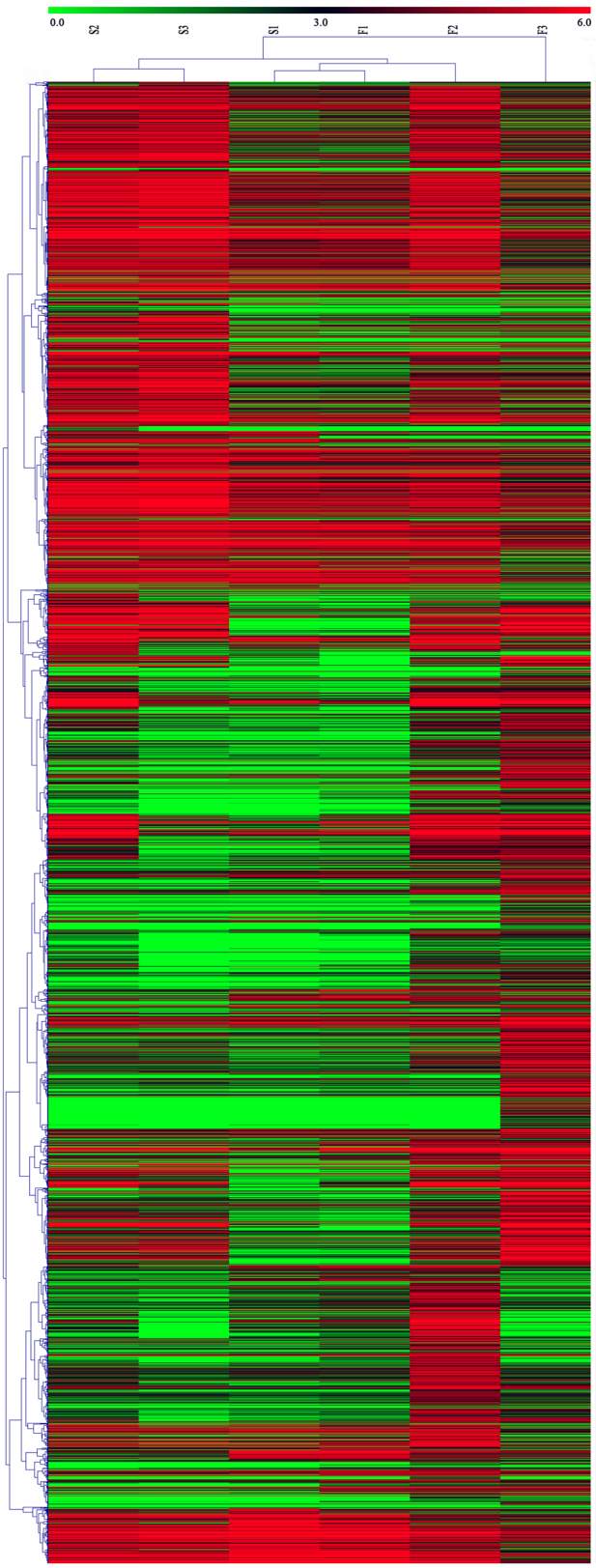

Fig. 4 Hierarchical clustering analysis of differentially expressed genes (DEGs) based on RPKM data. F1, F2 and F3 are samples of anther developmental stage PMA (pre-meiotic anther), MA (meiotic anther), and SCP (anthers with single celled pollen), respectively, for fertile buds, and S1, S2, and S3 are samples of the corresponding stages in sterile buds, respectively. The color key represents RPKM (reads per kilobase per million mapped reads) normalized log2 transformed counts. Red represents high expression and green represents low expression. Each row represents a gene (color figure online)

during MA and SCP stages ($p(X^2) < 0.001$). Furthermore, of the 43 down-regulated genes at the MA stage (Table 3), three genes were identified, whose orthologous genes were required for meiosis in *Arabidopsis*. They were *Bra004222*, *Bra035777*, and *Bra039753*, which were orthologous with *ASY1* (Wei and Zhang 2010), *MSH5* (Higgins et al. 2008) and *DUET/MMD1*(Andreuzza et al. 2015; Reddy et al. 2003; Wang et al. 2016b; Yang et al. 2003b), respectively. In particular, *DUET/MMD1* encoding a PHD finger protein is required for cell cycle transition and meiotic chromosome condensation during male meiosis (Andreuzza et al. 2015; Wang et al. 2016b). Meanwhile, *Bra038794*, orthologous with *TDM1* which is a direct target of *DUET/MMD1*, also exhibited down regulation at the MA stage (Table S1).

Expression analysis of genes for callose synthesis and dissolution

Callose is a linear β-1, 3-glucan molecule that plays significant roles in anther development. In this study, 17 genes related to callose synthesis were identified, among which, two were found related with callose synthesis and 15 with callose dissolution, which exhibited differential expression during the three stages of development under study in sterile anther (Table 4). *Bra028343*, homologous with *CALS5*, was the most important gene responsible for callose deposition surrounding meiocytes (Dong et al. 2005); the gene was significantly down-regulated in sterile flowers at both MAT and SCP stages. There were two, three, and eight genes involved in callose dissolution that were down-regulated at PAM, MAT, and SCP stage, respectively. Most noticeably of all, *A6*, whose expression level is a significant component of the callose mixture secreted by the tapetum, has 3 orthologous genes in *B. rapa*, *Bra032758*, *Bra037057*, and *Bra038969*. These 3 *BrA6* genes were all down-regulated in sterile flower buds at the SCP stage. In addition, we observed that *Bra004288*, orthologous with *CDM1*, showed a 35-fold transcript decline in sterile, compared with fertile flower buds at the MAT stage (Table S1).

Expression analysis of transcription factors (TF)

Transcriptional regulation is a major mechanism controlling differentiation of meiocytes and neighboring somatic

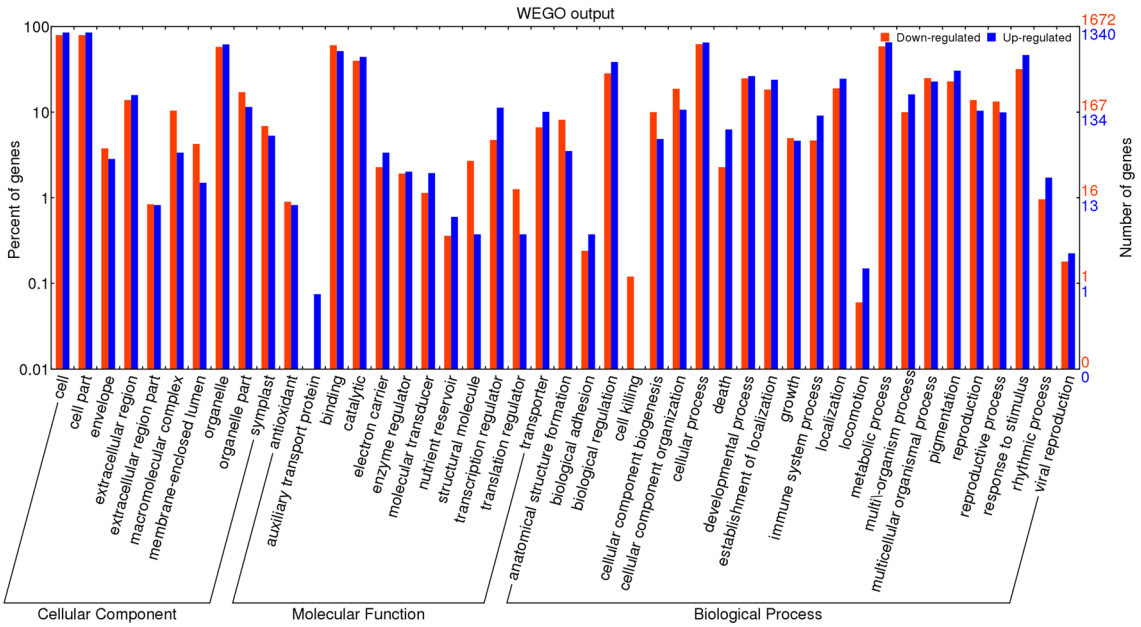

Fig. 5 GO analysis of differentially expressed genes. The x-axis indicates the sub-categories forming three main categories: cellular component, molecular function and biological process; the right y-axis indicates the number of DEGs in a sub-category and the left y-axis indicates the percentage of a specific category of genes in that main category

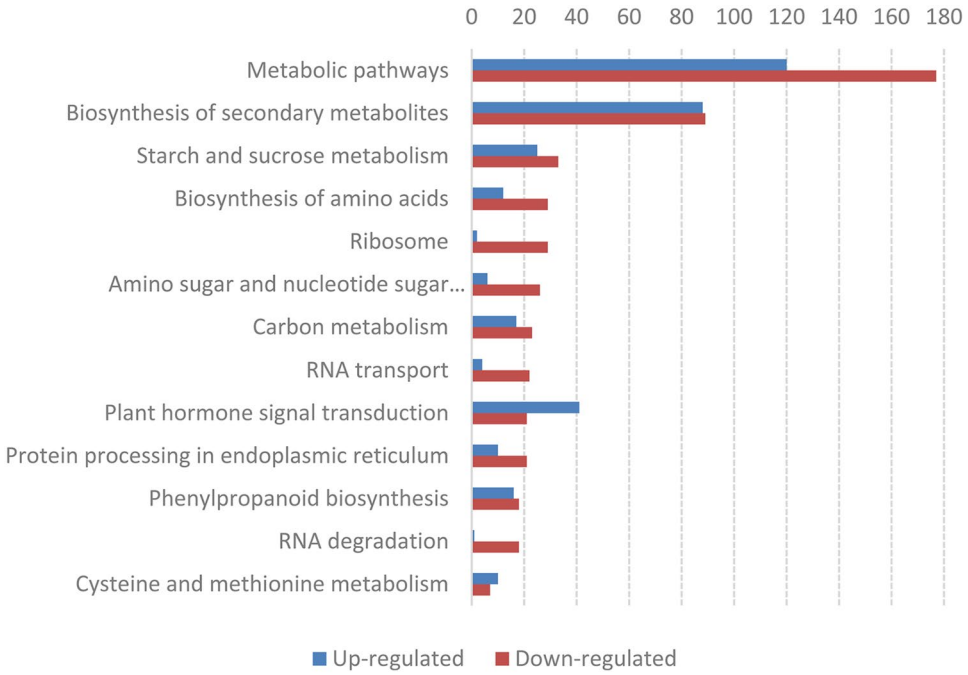

Fig. 6 The top 10 KEGG pathway categories in either up- or down- regulated genes. The x-axis indicates the number of DEGs in a sub-category and the y-axis indicates the categories of the KEGG pathway

tissues including tapetum during anther development (Ma 2006; Zhu et al. 2011).The list of *B. rapa* TF-genes, including 2502 putative TF genes classified into 57 TF families, were obtained from the Plant and Transcription Factor Database (http://planttfdb.cbi.pku.edu.cn/index.php). Based on RPKM, 252 genes of the 2502 putative TFs, accounting for 10.1% of total TF genes, showed significant differential expression in sterile buds compared with fertile buds during the three stages of anther development, PAM, MAT, and SCP (Table S2). The 252 TF genes came from 38 TF families and the top five TF families were NAC (43), MYB (22), ERF (21), bHLH (18), and C2H2 (18). Of all 252 TFs, there were 220, 28, and 4 accounting for 87.3%, 11.1%, and 1.6%, showing differential expression at one, two, and three anther

Table 3 Subset of genes related with meiosis highly expressing in Meiocyte

Br. gene ID	At. gene ID	Proposed function[a]	Gene model	Whether TF	Gene differential expression		
					S1 VS F1	S2 VS F2	S3 VS F3
Bra015379	AT1G05000	An atypical dual-specificity phosphatase	ATPFA-DSP1	No	–	–	↑
Bra030645	AT1G06250	Alpha/beta-Hydrolases superfamily protein		No	–	–	↓
Bra015486				No	↑	–	–
Bra031591	AT1G07750	RmlC-like cupins superfamily protein		No	–	–	↓
Bra030712	AT1G08050	Zinc finger (C3HC4-type RING finger) family protein		No	–	–	↓
Bra031688	AT1G09930	Oigopeptide transporter	ATOPT2, OPT2	No	–	↓	–
Bra018464	AT1G10060	Encodes a mitochondrial branched-chain amino acid aminotransferase	ATBCAT-1, BCAT-1	No	–	–	↓
Bra000672	AT1G14680	Unknown protein		No	–	↓	–
Bra026159	AT1G15190	Fasciclin-like arabinogalactan family protein		No	–	↓	–
Bra026144	AT1G15320	Unknown protein		No	–	↓	–
Bra026093	AT1G15920	Polynucleotidyl transferase, ribonuclease H-like superfamily protein		No	–	↓	–
Bra016393	AT1G22015	Transferase activity, transferring hexosyl groups, galactosyltransferase activity	DD46	No	–	–	↓
Bra030061	AT1G27720	Transcription initiation factor activity	TAF4, TAF4B,	No	–	↓	–
Bra010198	AT1G33430	Galactosyltransferase family protein		No	↑	–	–
Bra018702	AT1G36160	Encodes acetyl-CoA carboxylase	ACC1, EMB22, GK, SFR3	No	–	–	↓
Bra040305	AT1G44890	Homolog of yeast oxidase assembly 1 (OXA1)		No	–	–	↓
Bra018941	AT1G52030	Similar to myrosinase binding proteins which may be involved in metabolizing glucosinolates	F-ATMBP, MBP1.2, MBP2	No	–	↓	–
Bra002818				No	–	–	↓
Bra039753	AT1G66170	Encodes a PHD-domain containing protein required for male meiosis	DUET, MMD1	No	–	↓	–
Bra040627	AT1G66850	Bifunctional inhibitor/lipid-transfer protein/seed storage 2S albumin superfamily protein		No	↑	–	–
Bra004222	AT1G67370	ASY1 protein is initially distributed as numerous foci throughout the chromatin	ASY1, ATASY1	No	–	–	↓
Bra004316	AT1G68540	NAD(P)-binding Rossmann-fold superfamily protein, sporopollenin biosynthetic process	CCRL6,TKPR2	No	–	–	↓
Bra008822				No	↑	–	↓
Bra004386	AT1G69500	Encodes a cytochrome P450, designated CYP704B1. Expressed in the developing anthers	CYTOCHROME P450	No	–	–	↓
Bra004394	AT1G69560	Encodes LOF2, a MYB-domain transcription factor expressed in organ boundaries.	ATMYB105, LOF2	MYB	–	–	↓
Bra016021	AT1G73050	Glucose-methanol-choline (GMC) oxidoreductase family protein		No	–	↓	–
Bra015955	AT1G73890	Bifunctional inhibitor/lipid-transfer protein/seed storage 2S albumin superfamily protein		No	↓	↓	–
Bra015887	AT1G74870	RING/U-box superfamily protein		No	–	↓	–
Bra003728	AT1G76250	Unknown protein		No	–	↓	–

Table 3 (continued)

Br. gene ID	At. gene ID	Proposed function[a]	Gene model	Whether TF	Gene differential expression		
					S1 VS F1	S2 VS F2	S3 VS F3
Bra015649	AT1G77860	Seven-Path Transmembrane Protein;Mutant has Altered morphology of pollen exine wall	KOM, KOMPEITO	No	–	↓	–
Bra003610	AT1G79450	ALA-interacting subunit 5 (ALIS5)	ALIS5	No	–	–	↓
Bra035205	AT1G79900	Encodes a mitochondrial ornithine transporter that exports ornithine from the mitochondria to the cytosol	ATMBAC2, BAC2	No	–	–	↑
Bra008491	AT1G80160	Lactoylglutathione lyase/glyoxalase I family protein	GLYI7, GLYOXYLASE I 7	No	–	–	↑
Bra037213	AT2G13680	Responsible for the synthesis of callose deposited at the primary cell wall of meiocytes, tetrads and microspores	ATGSL02, CALS5, GLS2,	No	–	↓	↓
Bra013041	AT2G16910	Encodes a basic helix-loop helix transcription factor involved in tapetal cell development	AMS	bHLH	↑	–	↓
Bra002004				bHLH	↑	–	–
Bra002078	AT2G17700	ACT-like protein tyrosine kinase family protein	STY8	No	–	↓	–
Bra024476	AT2G18260	Member of SYP11 Gene Family	ATSYP112, SYP112	No	–	↓	–
Bra039622				No	–	↓	↓
Bra000527	AT2G27035	Has been classified as a stellacyanin. Has also been classified as an early nodulin-like protein (ENODL)	ATENODL20, ENODL20	No	↓	↓	–
Bra021598	AT2G29940	ATPase activity, coupled to transmembrane movement of substances	ATPDR3, PDR3	No	–	↓	↓
Bra022834	AT2G31270	Encodes a cyclin-dependent protein kinase. Involved in nuclear DNA replication and plastid division	ATCDT1A, CDT1, CDT1A	No	–	↓	–
Bra018272				No	–	–	↓
Bra022879	AT2G32235	Unknown protein		No	–	↓	–
Bra005574				No	–	↓	–
Bra005585	AT2G32350	Ubiquitin-like superfamily protein		No	–	↓	–
Bra005385	AT2G34870	Embryo development ending in seed dormancy	MEE26	No	–	↓	–
Bra005089	AT2G38690	Unknown protein		No	–	↓	–
Bra037635	AT2G44770	ELMO/CED-12 family protein		No	–	↓	–
Bra039319	AT2G45750	S-adenosyl-L-methionine-dependent methyltransferases superfamily protein		No	–	–	↓
Bra004933				No	↑	–	↓
Bra001051	AT3G02555	Unknown protein		No	–	–	↑
Bra001110	AT3G04620	Arget promoter of the male germline-specific transcription factor DUO1	DAN1	No	–	↓	↓
Bra010003				No	–	–	↓
Bra036129				No	–	–	↓
Bra040393				No	–	↓	–
Bra029644	AT3G07390	Extracellular matrix structural constituent	AIR12	No	–	–	↑
Bra013979	AT3G13280	Putative endonuclease or glycosyl hydrolase		No	–	–	↓
Bra027437	AT3G13420	Unknown protein		No	–	↓	–
Bra027246	AT3G15400	Encodes a protein with novel repeat sequences and a petunia glycine-rich cell wall protein	ANTHER 20, ATA20	No	–	–	↓
Bra027167	AT3G16380	Polyadenylate-binding protein	PAB6	No	–	↓	↓

Table 3 (continued)

Br. gene ID	At. gene ID	Proposed function[a]	Gene model	Whether TF	Gene differential expression		
					S1 VS F1	S2 VS F2	S3 VS F3
Bra035777	AT3G20475	A homologue of the MutS-homolog family, Involved in meiotic recombination	ATMSH5, MSH5	No	–	↓	–
Bra032986	AT3G27190	One of the homologous genes predicted to encode proteins with UPRT domains	UKL2	No	–	↓	–
Bra028324	AT3G42960	Arabidopsis homolog of TAS-SELSEED2. Expressed specifically in tapetal cells	ASD, ATA1, TA1	No	–	–	↓
Bra029913	AT3G48690	Encodes a protein with carboxylesterase whose activity was tested using both pNA and 2,4-D-methyl	ATCXE12, CXE12	No	–	–	↓
Bra012819	AT3G52130			No	↑	–	–
Bra006901		Lipid binding		No	↑	–	–
Bra014734	AT3G55570	Unknown protein		No	↑	–	–
Bra003281	AT3G55780	Glycosyl hydrolase superfamily protein		No	–	↓	–
Bra007190				No	–	↓	–
Bra014630	AT3G57370	Member of the TFIIB-related protein family, involved in regulation of the mitotic cell-cycle progression	BRP4	No	–	↓	–
Bra003279	AT3G57390	Encodes a MADS-box containing protein likely to be a transcription factor	AGL18	No	–	–	↓
Bra003380	AT3G59510	Leucine-rich repeat (LRR) family protein; INVOLVED IN: signal transduction		No	–	–	↓
Bra014536	AT3G59530	Calcium-dependent phosphotriesterase superfamily protein	ATLAP3, LAP3	No	–	–	↓
Bra007457				No	↑	–	–
Bra003475	AT3G61810	Glycosyl hydrolase family 17 protein		No	–	↓	–
Bra029430	AT4G12000	SNARE associated Golgi protein family		No	–	–	↑
Bra034880	AT4G13345	INVOLVED IN: embryo development ending in seed dormancy	MEE55	No	–	↑	–
Bra032758	AT4G14080	Maternal effect embryo arrest 48 (MEE48)	MEE48	No	–	–	↓
Bra037057				No	↑	–	↓
Bra038969				No	–	–	↓
Bra026359	AT4G27330	Encodes a putative transcription factor that is required for the initiation of both micro- and megagametogenesis	NOZZLE, NZZ, SPL	NZZ/SPL	–	–	↓
Bra019052	AT4G27410	Encodes a NAC transcription factor induced in response to desiccation	ATRD26, RD26	NAC	–	–	↑
Bra019048				No	–	–	↑
Bra034672	AT4G35070	SBP (S-ribonuclease binding protein) family protein		No	–	–	↓
Bra010535	AT4G35420	Encodes DRL1, a closely related homolog of the rice anther-specific gene OsDFR2	DRL1,TKPR1	No	–	–	↓
Bra005913	AT5G06820	Protein serine/threonine kinase activity, kinase activity, ATP binding	SRF2	No	–	↓	–
Bra009231				No	–	↓	–
Bra023394	AT5G13170	Encodes a member of the SWEET sucrose efflux transporter family proteins	ATSWEET15, SAG29	No	↑	–	↑
Bra008850				No	–	–	↑

Table 3 (continued)

Br. gene ID	At. gene ID	Proposed function[a]	Gene model	Whether TF	Gene differential expression		
					S1 VS F1	S2 VS F2	S3 VS F3
Bra006452	AT5G18320	ARM repeat superfamily protein; FUNCTIONS IN: ubiquitin-protein ligase activity		No	–	↓	–
Bra009707	AT5G23750	Remorin family protein		No	–	–	↑
Bra009761	AT5G24420	Encodes a cytosolic 6-phosphogluconolactonase thought to be involved in the oxidative pentose-phosphate pathway	PGL5	No	–	–	↓
Bra009795	AT5G24820	Eukaryotic aspartyl protease family protein; FUNCTIONS IN: aspartic-type endopeptidase activity		No	↑	–	–
Bra036584	AT5G26730	Fasciclin-like arabinogalactan family protein; FUNCTIONS IN: molecular_function unknown		No	↑	–	–
Bra025460	AT5G41800	Transmembrane amino acid transporter family protein; amino acid transmembrane transporter activity		No	–	–	↓
Bra028513	AT5G41890	Enzyme group with broad substrate specificity that may catalyze acyl transfer or hydrolase reactions with lipid and non-lipid substrates		No	–	↓	–
Bra033736	AT5G44330	Tetratricopeptide repeat (TPR)-like superfamily protein		No	–	↓	–
Bra033750	AT5G44540	Tapetum specific protein TAP35/TAP44		No	↑	–	–
Bra027558				No	↑	–	–
Bra039515				No	↑	–	↓
Bra022551	AT5G51480	Oxidoreductase activity, copper ion binding; INVOLVED IN: oxidation reduction	SKS2, SKU5 SIMILAR 2	No	–	–	↑
Bra029171				No	–	↓	↓
Bra022571	AT5G51950	Glucose-methanol-choline (GMC) oxidoreductase family protein; aldehyde-lyase activity, oxidoreductase activity		No	–	–	↓
Bra029151				No	–	–	↓
Bra028286				No	–	–	↓
Bra028294	AT5G52160	Bifunctional inhibitor/lipid-transfer protein/seed storage 2S albumin superfamily protein, INVOLVED IN: lipid transport;		No	↑	–	–
Bra022636	AT5G53190	Nodulin MtN3 family protein	ATSWEET3, SWEET3	No	↑	–	↓
Bra003075				No	–	–	↓
Bra022692	AT5G54080	Encodes a homogentisate 1,2-dioxygenase and is likely to be involved in tyrosine catabolism.	ATHGO, HGO	No	–	–	↑
Bra002891	AT5G55590	Encodes a protein with pectin methylesterase activity.	QRT1, QUARTET 1	No	–	–	↓
Bra024341	AT5G64960	Part of a CDKC kinase complex	CDKC2, CDKC2	No	–	↓	–

"↓", "↑" and "–" represent downregulation, upregulation and no significant difference in sterile buds, respectively, compared with the fertile buds, *F1, F2* and *F3* fertile samples of three distinct stages, pre-meiotic anther (PMA), meiotic anther (MA) and anthers with single celled pollen (SCP), respectively, *S1, S2* and *S3* samples of corresponding stage in sterile buds, respectively

[a]All the proposed function informations obtained from TAIR website (http://www.arabidopsis.org/)

developmental stage, respectively. *Bra023927*, the only EIL TF among 252 TFs, was up-regulated during all three stages. Interestingly, MYB-related TFs, *Bra004503*, *Bra030496*, and *Bra033291* were all down-regulated during all three stages. At MAT stage, 4 MYB TFs, *Bra005597*, *Bra012337*, *Bra026281*, and *Bra037828* were all up-regulated. In

Table 4 Subset of genes related with callose synthesis and dissolution

Callose metabolism	Br. gene ID	At. gene ID	Gene model	Proposed function[a]	Gene differential expression		
					S1 VS F1	S2 VS F2	S3 VS F3
Callose synthesis	Bra037213	AT2G13680	GLS2/CALS5	Responsible for the synthesis of callose deposited at the primary cell wall of meiocytes, tetrads and microspores	–	↓	↓
	Bra015436	AT1G05570	GLS6/CALS1	Encoding the cell plate-specific, callose synthase catalytic subunit	–	–	↑
Callose degradation	Bra000508	AT2G27500		Glycosyl hydrolase superfamily protein	–	–	↑
	Bra001918	AT3G23770		O-Glycosyl hydrolases family 17 protein	–	–	↓
	Bra014979			O-Glycosyl hydrolases family 17 protein	–	–	↓
	Bra028343			O-Glycosyl hydrolases family 17 protein	↓	–	↓
	Bra003281	AT3G55780		Glycosyl hydrolase superfamily protein	–	↓	–
	Bra007190			Glycosyl hydrolase superfamily protein	–	↓	–
	Bra003273	AT3G57240	BG3	A member of glycosyl hydrolase family 17	↓	–	–
	Bra003475	AT3G61810		Glycosyl hydrolase family 17 protein	–	↓	–
	Bra032758	AT4G14080	A6/MEE48	O-Glycosyl hydrolases family 17 protein	–	–	↓
	Bra037057		A6/MEE48	O-Glycosyl hydrolases family 17 protein	↑	–	↓
	Bra038969		A6/MEE48	O-Glycosyl hydrolases family 17 protein	–	–	↓
	Bra033549	AT4G16260		Encodes a putative beta-1,3-endoglucanase that interacts with the 30C02 cyst nematode effector	–	↑	↑
	Bra017659	AT4G34480		O-Glycosyl hydrolases family 17 protein	–	–	↑
	Bra002927	AT5G55180		O-Glycosyl hydrolases family 17 protein	–	–	↓
	Bra037795	AT5G64790		O-Glycosyl hydrolases family 17 protein	–	–	↓

"↓", "↑" and "–" represent downregulation, upregulation and no significant difference in sterile buds, respectively, compared with the fertile buds, *F1, F2* and *F3* fertile samples of three distinct stages, pre-meiotic anther (PMA), meiotic anther (MA) and anthers with single celled pollen (SCP), respectively, *S1, S2* and *S3* samples of corresponding stage in sterile buds, respectively

[a]All the proposed function informations obtained from TAIR website (http://www.arabidopsis.org/)

addition, *Bra013519* and *Bra025337*, orthologous with *DYT1*, encoding bHLH TF, and *TDF1*, encoding a putative R2R3 MYB TF, were down-regulated at the MAT stage in sterile buds. Concomitantly, all 7 C_3H TFs were down-regulated, including the three genes, *Bra004288*, *Bra030148*, and *Bra038204*, at the MAT stage and 4 genes, *Bra006465*, *Bra020750*, *Bra025776*, and *Bra040220*, at the SCP stage.

Validation of transcriptomics data by quantitative Real-Time PCR

To verify the reliability of our transcriptome sequencing results, expression analysis of ten sterility-related genes selected randomly from the transcriptome was performed by qPCR (Fig. 7). These ten genes were down-regulated in sterile line of WS24-3A. Two genes of *Bra033736* and *Bra007457* were down-regualted in sterile line at MAT stage. Four genes of *Bra007577*, *Bra002401*, *Bra038969* and *Bra027246* were down-regualted in sterile line at SCP stage. *Bra028343*, *Bra034793* and *Bra013041* were lowly expressed in WS24-3A at PMA stage and SCP stage. *Bra028969* was further validated for all the three stages. The

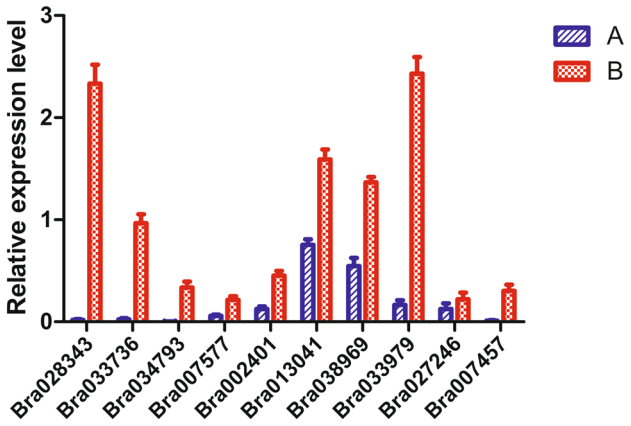

Fig. 7 qPCR analysis of sterility-related genes selected randomly. A shows sterile plant (blue), B represents fertile plants (red). Error bars indicate standard error (color figure online)

expression levels of the ten genes displayed the same trend as the transcriptome sequencing results. These consequences ensured the high reliability of the RNA-seq data obtained in the present study.

Discussion

In this study, abnormal development and differentiation of both meiocyte and tapetal cells were observed in sterile anthers of WS24-3A (Figs. 1, 2). No tetrads were produced during or after stage 7 (Fig. 1i, j, l), and tapetal cells failed to convert to secretory cells, thus leading to delayed degradation of the callose wall in anthers of WS24-3A (Fig. 2g, h). These abnormalities differed from the defective phenotype of reported recessive genic-sterile lines in *Brassica* crops (Dun et al. 2011; Yi et al. 2010; Zhou et al. 2012). S45A and 7365A were both recessive genic-sterile lines of *Brassica napus*. Meiocytes of male sterile mutant S45A could complete meiosis to produce tetrads at stage 7, but the pattern of apoptosis in the tapetum was seriously defective, resulting in no pollen exine formation (Yi et al. 2010). Meiocytes of male sterile mutant 7365A completed meiosis to produce tetrads at stage 7, but tapetal cells exhibited abnormal enlargement at anther stage 6 and lost their secretory function during and after stage 7, resulting in abnormal microspore release (Dun et al. 2011; Zhou et al. 2012). Interestingly, a dominant genic-sterile line, FM195A, exhibited arrested meiotic chromosome during meiosis, and failed to produce tetrads. However, the dominant genic-sterile gene encoding FM195A, *MS5*^{b}, also affected the process of megasporogenesis, thus resulting in severely reduced female fertility, which was remarkably different from WS24-3A (Xin et al. 2016). No significant alterations were observed in the remaining three somatic layers before, during, or after stage 7 in WS24-3A. However, we cannot exclude the possibility that subtle alterations might have been presented or passed undetected. We also observed that the filaments were remarkably shorter in sterile flowers than those in fertile flowers (Fig. S1). This finding suggests that the sterile gene of WS24-3A, *Bra2ms*, might also play a minor role in flower development.

To obtain helpful information for further cloning of *Bra2ms*, RNA-seq was employed to perform a global comparative analysis between sterile and fertile flower buds in three stages of anther development, PMA, MA, and SCP. In sterile buds, 3282 DEGs, 2055 down-regulated and 1625 up-regulated, were identified during the three stages of anther development (Table S1). Based on our results of microsectioning, as no tetrads were observed, we focused on DEGs at the MA stage. There were 626 down-regulated DEGs, accounting for 69% of a total of 908 DEGs, whereas only 282 up-regulated DEGs were detected. Among the 626 down-regulated DEGs, we underlined genes required for male meiosis, callose synthesis and dissolution, and tapetum development, according to the annotation of orthologous genes in *Arabidopsis thaliana*. There were 44 DEGs, corresponding to 38 *Arabidopsis* genes (Table 3), accounting for 12.8% of a subset of genes preferentially expressed in meiocytes, including three genes, *ASY1* (Wei and Zhang 2010), *MSH5* (Higgins et al. 2008) and *DUET/MMD1* (Andreuzza et al. 2015; Wang et al. 2016b), that proved necessary for male meiosis (Libeau et al. 2011). These results were consistent with the observations of microsections, indicating that *Bra2MS* might function upstream of the male meiosis-related genes in meiocytes at stage 6, and play an important role in meiosis of meiocytes.

The orthologous genes of *Brassica rapa* functioning at an early stage and determining tapetal formation, such as *SPL/NZZ* (Schiefthaler et al. 1999), *BAM1* (DeYoung et al. 2006), *BAM2* (Hord et al. 2006), *EMS1/EXS* (Canales et al. 2002), *SERK1* (Albrecht et al. 2005), *SERK2* (Colcombet et al. 2005), and *TPD1* (Cifuentes et al. 2016; Huang et al. 2016; Yang et al. 2003a) did not show differential expression (Table S1), which indicated that the early formation and differentiation of tapetal cells were normal in anthers of WS24-3A. Significantly, *Bra013519* and *Bra025337*, orthologous with *DYT1*, were both down-regulated at the MA stage. *DYT1* acts downstream of *SPL* and upstream of *TDF1*, strongly expressed in the tapetum from late stage 5 to early stage 6, and a crucial component of a genetic network that regulates tapetum development. Meiocytes of mutant *dyt1* often failed to complete meiotic cytokinesis at stage 7 and the tapetum and middle layer cells gradually formed excess vacuolization during and after stage 6, which were similar and different with those in WS24-3A. We also found 17 related genes involved in callose synthesis and dissolution, including the orthologous genes of *CALS5* (Dong et al. 2005), *A6* (Hird et al. 1993), and *CDM1* (Lu et al. 2014), which showed differential expression during the three stages of anther development studied. Especially, *Bra004288*, orthologous with *CDM1* acting upstream of *CALS5* and *A6*, showed a 35-fold transcript decline in sterile anthers at the MAT stage (Table S1). Together, these results indicate that the early formation and differentiation of tapetal cells were normal before late stage 5, but further development of tapetum in WS24-3A was defective at and after stage 6. Defective tapetum development mainly reflected as a delay of the dissolution of the callose wall surrounding the miocyte after stage 7 (Fig. 2), which indicated that the tapetal cells failed to convert into secretory cells.

The mechanism controlling the specification and development of the tapetum and meiocytes within the anthers of WS24-3A remains a mystery. Although defective in tapetum development and meiocyte meiosis, *dyt1* and *duet1/mmd1*, both failed to produce tetrads, and the somatic cell layers were less affected between anther stage 6 and 10 in the *duet1/mmd1*mutant, which resembled the mutant phenotype of WS24-3A more closely.

Conclusion

Comparative transcript profiling revealed 3282 DEGs, 2055 down-regulated and 1625 up-regulated, during three stages of anther developmental: pre-meiotic anther, meiotic anther, and anthers with single-celled pollen. At the meiotic anther stage, 626 DEGs were down-regulated, accounting for 69% of DEGs, whereas only 282 were up-regulated at this stage. Furthermore, we identified a series of genes and transcription factors required for male meiosis, callose synthesis and dissolution, and tapetum development among down-regulated DEGs, which included three meiosis-related genes, *ASY1*, *MSH5*, and *DUET/MMD1*; three callose metabolism related genes, *CALS5*, *A6*, and *CDM1*; and two TFs necessary for early tapetum development, *DYT1* and *TDF1*; these observations agreed with the results obtained by microsectioning. *Bra2MS* might function upstream of the male meiosis-related genes in meiocytes at stage 6 and affect the transition of the tapetum to the secretory cell type in non-heading Chinese cabbage.

Together, our findings contribute to the understanding of the mechanism underlying male sterility and provide helpful information for further gene cloning of *Bra2ms* in WS24-3A.

Acknowledgements This study was supported by the Innovation Fund of Wuhan Academy of Agricultural Science and Technology (CX201719-03), the National Key Research and Development Program of China (2017YFD0101803), Bulk Vegetable Industry Technology Systems of China (CARS-23-G-26) and the Natural Science Foundation of Hubei Province Youth program (ZRMS2019001622). We thank anonymous reviewers very much for providing constructive comments.

Author contributions LS and XL contributed equally to this study. Conceptualization, LS; Formal analysis, XL and FZ; Investigation, LS and XL; Methodology, LS and FZ; Resources, AW; Supervision, AW, CG, BW, CL, JT and GZ; Visualization, LS; writing—original draft, LS and XL; writing—review and editing, JT and GZ.

Compliance with ethical standards

Conflict of interest The authors declare no conflict of interest, financial or otherwise.

Human and animal rights No animals/humans were used for studies that are base of this research.

References

Akter S, Huq MA, Jung YJ, Cho YG, Kang KK (2016) Application of single nucleotide polymorphism markers for selection of male sterility in crop plants. Plant Breed Biotech 4:379–386

Albrecht C, Russinova E, Hecht V, Baaijens E, de Vries S (2005) The *Arabidopsis thaliana* SOMATIC EMBRYOGENESIS RECEPTOR-LIKE KINASES1 and 2 control male sporogenesis. Plant Cell 17:3337–3349

Andreuzza S, Nishal B, Singh A, Siddiqi I (2015) The chromatin protein DUET/MMD1 controls expression of the meiotic gene TDM1 during male meiosis in Arabidopsis. PLoS Genet 11:e1005396

Ashburner M, Ball CA, Blake JA, Botstein D, Butler H, Cherry JM, Davis AP, Dolinski K, Dwight SS, Eppig JT et al (2000) Gene ontology: tool for the unification of biology. The Gene Ontology Consortium. Nat Genet 25:25–29

Bohra A, Jha UC, Adhimoolam P, Bisht D, Singh NP (2016) Cytoplasmic male sterility (CMS) in hybrid breeding in field crops. Plant Cell Rep 35:967–993

Canales C, Bhatt AM, Scott R, Dickinson H (2002) EXS, a putative LRR receptor kinase, regulates male germline cell number and tapetal identity and promotes seed development in Arabidopsis. Curr Biol 12:1718–1727

Chang F, Wang Y, Wang S, Ma H (2011) Molecular control of microsporogenesis in Arabidopsis. Curr Opin Plant Biol 14:66–73

Chang L, Liu Z, Li C, Yun Z, Hui F (2016) Comparative transcriptome analysis of fertile and sterile buds from a genetically male sterile line of Chinese cabbage. Vitro Cell Dev Biol Plant 52:130–139

Chen G, Ye X, Zhang S, Zhu S, Yuan L, Hou J, Wang C (2018) Comparative transcriptome analysis between fertile and CMS flower buds in Wucai (*Brassica campestris* L.). BMC Genom 19:908

Cifuentes M, Jolivet S, Cromer L, Harashima H, Bulankova P, Renne C, Crismani W, Nomura Y, Nakagami H, Sugimoto K et al (2016) TDM1 regulation determines the number of meiotic divisions. Plos Genet 12:e1005856

Colcombet J, Boisson-Dernier A, Ros-Palau R, Vera CE, Schroeder JI (2005) Arabidopsis SOMATIC EMBRYOGENESIS RECEPTOR KINASES1 and 2 are essential for tapetum development and microspore maturation. Plant Cell 17:3350–3361

Cui J, You C, Zhu E, Huang Q, Ma H, Chang F (2016) Feedback regulation of DYT1 by interactions with downstream bHLH factors promotes DYT1 nuclear localization and anther development. Plant Cell 28:1078–1093

DeYoung BJ, Bickle KL, Schrage KJ, Muskett P, Patel K, Clark SE (2006) The CLAVATA1-related BAM1, BAM2 and BAM3 receptor kinase-like proteins are required for meristem function in Arabidopsis. Plant J 45:1–16

Dong X, Hong Z, Sivaramakrishnan M, Mahfouz M, Verma DP (2005) Callose synthase (CalS5) is required for exine formation during microgametogenesis and for pollen viability in Arabidopsis. Plant J 42:315–328

Dun X, Zhou Z, Xia S, Wen J, Yi B, Shen J, Ma C, Tu J, Fu T (2011) BnaC. Tic40, a plastid inner membrane translocon originating from *Brassica oleracea*, is essential for tapetal function and microspore development in *Brassica napus*. Plant J 68:532–545

Feng X, Dickinson HG (2010) Cell-cell interactions during patterning of the Arabidopsis anther. Biochem Soc Trans 38:571–576

Feng BM, Lu DH, Ma X, Peng YB, Sun YJ, Ning G, Ma H (2012) Regulation of the Arabidopsis anther transcriptome by DYT1 for pollen development. Plant J 72:612–624

Fu Z, Yu J, Cheng X, Zong X, Xu J, Chen M, Li Z, Zhang D, Liang W (2014) The rice basic helix-loop-helix transcription factor TDR INTERACTING PROTEIN2 is a central switch in early anther development. Plant Cell 26:1512–1524

Glover J, Grelon M, Craig S, Chaudhury A, Dennis E (1998) Cloning and characterization of MS5 from Arabidopsis: a gene critical in male meiosis. Plant J 15:345–356

Goldberg RB, Beals TP, Sanders PM (1993) Anther development: basic principles and practical applications. Plant Cell 5:1217–1229

Gotz S, Garcia-Gomez JM, Terol J, Williams TD, Nagaraj SH, Nueda MJ, Robles M, Talon M, Dopazo J, Conesa A (2008) High-throughput functional annotation and data mining with the Blast2GO suite. Nucleic Acids Res 36:3420–3435

Hafidh S, Fila J, Honys D (2016) Male gametophyte development and function in angiosperms: a general concept. Plant Reprod 29:31–51

Higgins JD, Vignard J, Mercier R, Pugh AG, Franklin FC, Jones GH (2008) AtMSH5 partners AtMSH4 in the class I meiotic crossover pathway in *Arabidopsis thaliana*, but is not required for synapsis. Plant J 55:28–39

Hird DL, Worrall D, Hodge R, Smartt S, Paul W, Scott R (1993) The anther-specific protein encoded by the *Brassica napus* and *Arabidopsis thaliana* A6 gene displays similarity to beta-1,3-glucanases. Plant J 4:1023–1033

Hord CLH, Chen CB, DeYoung BJ, Clark SE, Ma H (2006) The BAM1/BAM2 receptor-like kinases are important regulators of Arabidopsis early anther development. Plant Cell 18:1667–1680

Huang J, Zhang T, Linstroth L, Tillman Z, Otegui MS, Owen HA, Zhao D (2016) Control of anther cell differentiation by the small protein ligand TPD1 and its receptor EMS1 in Arabidopsis. PLoS Genet 12:e1006147

Ito T, Wellmer F, Yu H, Das P, Ito N, Alves-Ferreira M, Riechmann JL, Meyerowitz EM (2004) The homeotic protein AGAMOUS controls microsporogenesis by regulation of SPOROCYTELESS. Nature 430:356–360

Kanehisa M, Araki M, Goto S, Hattori M, Hirakawa M, Itoh M, Katayama T, Kawashima S, Okuda S, Tokimatsu T et al (2008) KEGG for linking genomes to life and the environment. Nucleic Acids Res 36:D480–D484

Li X, Wang A, Zu F, Hu Z, Lin J, Zhou G, Tu J (2016) Identification of a nuclear-recessive gene locus for male sterility on A2 chromosome using the Brassica 60 K SNP array in non-heading Chinese cabbage. Genes & Genom 38:1151–1157

Li DD, Xue JS, Zhu J, Yang ZN (2017) Gene regulatory network for tapetum development in *Arabidopsis thaliana*. Front Plant Sci 8:1559

Libeau P, Durandet M, Granier F, Marquis C, Berthome R, Renou JP, Taconnat-Soubirou L, Horlow C (2011) Gene expression profiling of Arabidopsis meiocytes. Plant Biol (Stuttg) 13:784–793

Lu P, Chai M, Yang J, Ning G, Wang G, Ma H (2014) The Arabidopsis CALLOSE DEFECTIVE MICROSPORE1 gene is required for male fertility through regulating callose metabolism during microsporogenesis. Plant Physiol 164:1893–1904

Ma H (2006) A molecular portrait of Arabidopsis meiosis. Arabidopsis Book 4:e0095

Ma H (2013) A battle between genomes in plant male fertility. Nat Genet 45:472–473

Parish RW, Li SF (2010) Death of a tapetum: a programme of developmental altruism. Plant Sci 178:73–89

Reddy TV, Kaur J, Agashe B, Sundaresan V, Siddiqi I (2003) The DUET gene is necessary for chromosome organization and progression during male meiosis in Arabidopsis and encodes a PHD finger protein. Development 130:5975–5987

Sanders PM, Bui AQ, Weterings K, McIntire KN, Hsu Y-C, Lee PY, Truong MT, Beals TP, Goldberg RB (1999) Anther developmental defects in *Arabidopsis thaliana* male-sterile mutants. Sexual Plant Reprod 11:297–322

Schiefthaler U, Balasubramanian S, Sieber P, Chevalier D, Wisman E, Schneitz K (1999) Molecular analysis of NOZZLE, a gene involved in pattern formation and early sporogenesis during sex organ development in *Arabidopsis thaliana*. Proc Natl Acad Sci USA 96:11664–11669

Scott RJ, Spielman M, Dickinson HG (2004) Stamen structure and function. Plant Cell 16(Suppl):S46–S60

Trapnell C, Williams BA, Pertea G, Mortazavi A, Kwan G, van Baren MJ, Salzberg SL, Wold BJ, Pachter L (2010) Transcript assembly and quantification by RNA-Seq reveals unannotated transcripts and isoform switching during cell differentiation. Nat Biotechnol 28:511-U174

Trapnell C, Roberts A, Goff L, Pertea G, Kim D, Kelley DR, Pimentel H, Salzberg SL, Rinn JL, Pachter L (2012) Differential gene and transcript expression analysis of RNA-seq experiments with TopHat and Cufflinks. Nat Protoc 7:562–578

Wang D, Guo Y, Wu C, Yang G, Li Y, Zheng C (2008) Genome-wide analysis of CCCH zinc finger family in Arabidopsis and rice. BMC Genomics 9:44

Wang LK, Feng ZX, Wang X, Wang XW, Zhang XG (2010) DEGseq: an R package for identifying differentially expressed genes from RNA-seq data. Bioinformatics 26:136–138

Wang X, Wang H, Wang J, Sun R, Wu J, Liu S, Bai Y, Mun JH, Bancroft I, Cheng F et al (2011) The genome of the mesopolyploid crop species Brassica rapa. Nat Genet 43:1035–1039

Wang A, Hu J, Huang X, Li X, Zhou G, Yan Z (2016a) Comparative transcriptome analysis reveals heat-responsive genes in Chinese cabbage (*Brassica rapa* ssp. chinensis). Front Plant Sci 7:939

Wang J, Niu B, Huang J, Wang H, Yang X, Dong A, Makaroff C, Ma H, Wang Y (2016b) The PHD finger protein MMD1/DUET ensures the progression of male meiotic chromosome condensation and directly regulates the expression of the condensin gene CAP-D3. Plant Cell 28:1894–1909

Wei F, Zhang GS (2010) Meiotically asynapsis-induced aneuploidy in autopolyploid *Arabidopsis thaliana*. J Plant Res 123:87–95

Xie C, Mao XZ, Huang JJ, Ding Y, Wu JM, Dong S, Kong L, Gao G, Li CY, Wei LP (2011) KOBAS 2.0: a web server for annotation and identification of enriched pathways and diseases. Nucleic Acids Res 39:W316–W322

Xin Q, Shen Y, Li X, Lu W, Wang X, Han X, Dong FM, Wan LL, Yang GS, Hong DF et al (2016) MS5 mediates early meiotic progression and its natural variants may have applications for hybrid production in *Brassica napus*. Plant Cell 28:1263–1278

Yang SL, Xiea LF, Mao HZ, Puah CS, Yang WC, Jiang LX, Sundaresan V, Ye D (2003a) TAPETUM DETERMINANT1 is required for cell specialization in the Arabidopsis anther. Plant Cell 15:2792–2804

Yang X, Makaroff CA, Ma H (2003b) The Arabidopsis MALE MEIOCYTE DEATH1 gene encodes a PHD-finger protein that is required for male meiosis. Plant Cell 15:1281–1295

Ye J, Fang L, Zheng HK, Zhang Y, Chen J, Zhang ZJ, Wang J, Li ST, Li RQ, Bolund L et al (2006) WEGO: a web tool for plotting GO annotations. Nucleic Acids Res 34:W293–W297

Yi B, Zeng F, Lei S, Chen Y, Yao X, Zhu Y, Wen J, Shen J, Ma C, Tu J et al (2010) Two duplicate CYP704B1-homologous genes BnMs1 and BnMs2 are required for pollen exine formation and tapetal development in *Brassica napus*. Plant J 63:925–938

Zhang D, Yang L (2014) Specification of tapetum and microsporocyte cells within the anther. Curr Opin Plant Biol 17:49–55

Zhang W, Sun YJ, Timofejeva L, Chen CB, Grossniklaus U, Ma H (2006) Regulation of Arabidopsis tapetum development and function by dysfunctional tapetum1 (dyt1) encoding a putative bHLH transcription factor. Development 133:3085–3095

Zhao D (2009) Control of anther cell differentiation: a teamwork of receptor-like kinases. Sex Plant Reprod 22:221–228

Zhou Z, Dun X, Xia S, Shi D, Qin M, Yi B, Wen J, Shen J, Ma C, Tu J et al (2012) BnMs3 is required for tapetal differentiation and degradation, microspore separation, and pollen-wall biosynthesis in *Brassica napus*. J Exp Bot 63:2041–2058

Zhu J, Chen H, Li H, Gao JF, Jiang H, Wang C, Guan YF, Yang ZN (2008) Defective in Tapetal development and function 1 is essential for anther development and tapetal function for microspore maturation in Arabidopsis. Plant J 55:266–277

Zhu J, Lou Y, Xu X, Yang ZN (2011) A genetic pathway for tapetum development and function in Arabidopsis. J Integr Plant Biol 53:892–900

Zhu EG, You CJ, Wang SS, Cui J, Niu BX, Wang YX, Qi J, Ma H, Chang F (2015) The DYT1-interacting proteins bHLH010, bHLH089 and bHLH091 are redundantly required for Arabidopsis anther development and transcriptome. Plant J 83:976–990

Affiliations

Liping Song[1] · Xia Li[3] · Feng Zu[4] · Changbin Gao[1] · Bincai Wang[1] · Chufa Lin[1] · Jinxing Tu[2] · Aihua Wang[1] · Guolin Zhou[1]

Liping Song
lp19871120@126.com

Xia Li
lixia_napus@163.com

Feng Zu
zufeng1984@163.com

Changbin Gao
gaocb1983@163.com

Bincai Wang
2858810879@qq.com

Chufa Lin
cflin3228@sina.com

Jinxing Tu
tujx@mail.hzau.edu.cn

[1] Wuhan Vegetable Research Institute, Wuhan Academy of Agriculture Science and Technology, Wuhan 430345, China

[2] National Key Laboratory of Crop Genetic Improvement, National Center of Rapeseed Improvement in Wuhan, Huazhong Agricultural University, Wuhan 430070, China

[3] Biotechnology and Genetic Resources Institute, Yunnan Academy of Agricultural Sciences, Kunming, People's Republic of China

[4] Industrial Crops Institute, Yunnan Academy of Agricultural Sciences, Kunming, People's Republic of China